

# CLOUD-ASSISTED INDIVIDUAL $L_1$ -PCA FACE RECOGNITION USING WAVELET-DOMAIN COMPRESSED IMAGES

Federica Maritato\*, Ying Liu<sup>+</sup>, Stefania Colonnese\*, and Dimitris A. Pados<sup>+</sup>

\*Department of Information Engineering, Electronics and Telecommunications,  
La Sapienza University of Rome, Rome, 00185 Italy,

<sup>+</sup>Department of Electrical Engineering,  
The State University of New York at Buffalo, Buffalo, NY 14260 USA

## ABSTRACT

Face recognition has been an active research field for a long time, and recently new challenges have arisen in designing cloud-assisted face recognition algorithms. In a cloud-assisted face recognition system, mobile devices acquire the data images; then, in order to unbind the cloud face recognition algorithm from the particular features extracted at the mobile device, the images are encoded and uploaded into the cloud. In this framework, it is important to understand and control the effect of the image compression stage performed at the mobile device on the performances of the face recognition algorithms realized within the cloud. Here, we analyze the impact of wavelet domain image compression on the Individual Adaptive (IA)  $L_1$ -PCA subspace computation and assess the performance of a classifier operating on data characterized by increasing compactness and accordingly decreasing accuracy.

**Index Terms**— Cloud assisted, face recognition,  $L_1$ -PCA, wavelet.

## 1. INTRODUCTION

Face recognition has been an active research field for a long time, as testified by a huge literature [1], where Principal Component Analysis (PCA) and Linear Discriminant Analysis (LDA) play the lion role among holistic approaches. In particular, recent developments on the  $L_1$ -norm [2],[4], have yielded an  $L_1$ -PCA based algorithm representing the main features of a random face with a small number of  $L_1$ -PCA components and associating a new unknown face image to the  $L_1$ -nearest class in the database.

Thanks to  $L_1$ -norm outlier rejection property,  $L_1$ -PCA based algorithms [3] proved to be resilient in presence of partial occlusion of the test images. The Individual Adaptive  $L_1$ -PCA based face recognition algorithm was also developed in [5] where, given the total number of principal components, a different number of components is adaptively allocated to each of the dataset classes.

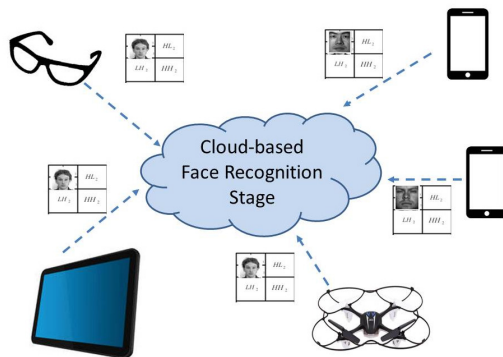


Fig. 1. Cloud-assisted Face Recognition Architecture.

Recently, due to the increasing interest in cloud-based services [6], the research on face recognition has found new challenges in designing algorithms suited for being realized by mobile devices connected to a network or to a cloud [7]. Fig. 1 represents an example of cloud-assisted face recognition architecture. In such framework, computationally heavy tasks as feature extraction and comparison with huge databases can be conveniently offloaded by the mobile device towards the cloud; then, in-cloud servers, possibly organized so as to minimize the time required for recognition [8], realize the recognition task.

In a cloud assisted face recognition system, after mobile devices have acquired the data images, they either compute and transmit the image features needed for classification or transmit the image itself. The first solution alleviates the amount of data to be transmitted from the mobile to the cloud; still, it requires a larger computational effort by the mobile device. More relevantly, it bounds the cloud face recognition algorithm to the particular feature extraction stage adopted at the mobile device, definitely limiting the actual recognition power left to the cloud.

Here, we consider the above described cloud-assisted recognition framework, and we address the case in which the image is compressed in the wavelet domain and then encoded and sent to the cloud, which in turn could implement different techniques and choose the one providing better distinctiveness between different classes. In this framework, it is important to understand and control the effect of the image compression stage performed at the mobile device on the performances of the face recognition algorithms realized within the cloud. Here, we focus on the impact of wavelet domain image compression on the Individual Adaptive (IA)  $L_1$ -PCA subspace computation [5] and we assess the performance of a classifier operating on data characterized by increasing compactness and accordingly decreasing accuracy.

The rest of the paper is organized as follows: in Sect. 2 we recall the wavelet domain signal model, in Sect. 3 performances on wavelet-domain compressed images, Sect. 4 shows the experimental studies on three face data sets. Conclusions and further research directions are illustrated in Sect. 5.

## 2. SIGNAL MODEL

Since the pioneering work [9], representation of a signal through a shaped oscillating wave with fast decay has found application in a variety of processing tasks. When applied to image compression, the Discrete Wavelet Transform [14] splits the image components into different subbands and allows to identify visually relevant information from each subband; therefore, it is adopted in encoding standard [10] as well as in different sparsity seeking image representation procedures [11].

The impact of different wavelet components on the discriminatory power of face recognition algorithms is studied in [12], where the authors analyze the application of LDA to study various facial features in spatial and wavelet domain or in [13] they study the LDA applied to face recognition problem the small sample size problem occurs.

Herein, we instead consider the effect on face recognition algorithm performances due to image compression. In fact, in a cloud-assisted face recognition system, the test images are acquired at the mobile device, and are firstly encoded and then uploaded into the cloud to offload the computation; wavelet domain image data reduction tightly models different image compression procedures performed at the mobile device.

Specifically, let us denote by  $\xi$  the  $D$ -dimensional vector representing the image under concern in lexicographic form, and by  $\mathbf{x}$  the  $D$ -dimensional vector representing its Discrete Wavelet Transform (DWT) obtained by recursive application of Daubechies filter [14]. In this domain, application of the Daubechies filter splits the image spectrum into four subbands the first of which, also known as LL subband, contains horizontal lows/vertical lows. Recursive application of

Daubechies filters on the LL subband obtains  $L > 2$  levels of decomposition of the original image into octave bands.

Fig. 2 shows the DWT of three face images from different databases using Daubechies filter and  $L_{max} = 2$  levels of decomposition.

In the following, we consider the case, illustrated in Fig. 3, in which the image a) is acquired, b) is decomposed into  $L_{max}$  octave bands, and image compression is realized by discarding the subbands relative to the  $l$ -th higher frequency layers, and (c) the residual  $L_{max} - l$  lower frequency DWT coefficients are sent.

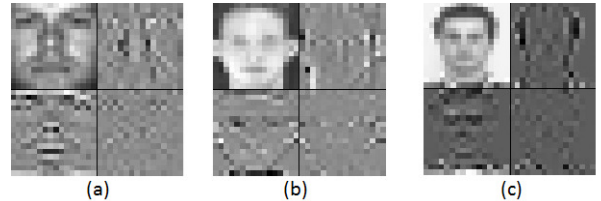


Fig. 2. A subject of Yale (a), ORL (b) and Aberdeen (c) database with its wavelet transform using Daubechies filter.

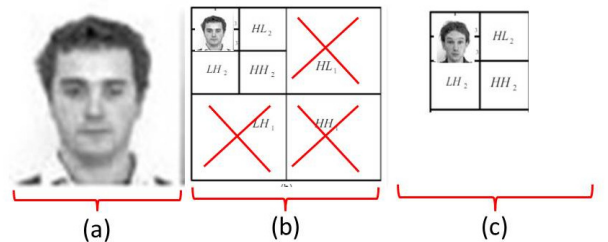


Fig. 3. Face recognition offloading: stages performed at the mobile device: (a) image acquisition, (b) image encoding wavelet domain data reduction, (c) encoded image uploading.

## 3. CLASSIFICATION USING WAVELET-DOMAIN REDUCED REPRESENTATION

Herein, we address the performance of the IA  $L_1$ -PCA Face Recognition algorithm in [5] on images encoded by discarding higher frequency layers in the wavelet domain. To this aim, let us here briefly recall the basics of IA  $L_1$ -PCA. Let  $C$  denote the number of classes, and let the  $j$ -th class be characterized with  $N$  training samples, represented by a  $D$ -dimensional vector  $\mathbf{x}_n^{(j)}$ ,  $n = 1, \dots, N$ . Let us then collect the

$N$  training samples of each class within a  $D \times N$  training matrix

$$\mathbf{X}^{(j)} = [\mathbf{x}_1^{(j)}, \mathbf{x}_2^{(j)}, \dots, \mathbf{x}_N^{(j)}], j = 1, \dots, C$$

The class training matrix is then zero-centered by subtracting the class sample-mean  $\boldsymbol{\mu}^{(j)} = \frac{1}{N}\mathbf{X}^{(j)}\mathbf{1}_N$ . The Individual  $L_1$ -PCA then envisages the evaluation of the class-related subspace as

$$\mathbf{Q}_{L_1}^{(j)} = \arg \max_{\substack{\mathbf{Q} \in \mathbb{Q}^{D \times K} \\ \mathbf{Q}^T \mathbf{Q} = \mathbf{I}}} \|\mathbf{X}^T \mathbf{Q}\|_1. \quad (1)$$

The classification stage of a test vector  $\mathbf{x}_t$  encompasses i) subtraction of the mean of the  $j$ -th class  $\boldsymbol{\mu}^{(j)}$  from  $\mathbf{x}_t$ , ii) projection of the zero-centered test data point onto the  $j$ -th  $L_1$  subspace  $\mathbf{Q}_{L_1}^{(j)}$ , iii) selection of the nearest class-related subspace. Thereby, the vector  $\mathbf{x}_t$  is classified as belonging to the  $\hat{j}_{I L_1}$  class, being  $\hat{j}_{I L_1}$  computed as

$$\hat{j}_{I L_1} = \arg \min_{1 \leq j \leq C} \left\| (\mathbf{x}_t - \boldsymbol{\mu}^j) - \mathbf{Q}_{L_1}^{(j)} \mathbf{Q}_{L_1}^{(j)T} (\mathbf{x}_t - \boldsymbol{\mu}^j) \right\|_2 \quad (2)$$

The Individual Adaptive  $L_1$ -PCA extends the above described Individual  $L_1$ -PCA by allocating a total number of  $K_C$  principal components to different classes allowing the computed  $L_1$ -subspace of different classes to have -possibly-different rank. The rank value  $K^{(j)}, j = 1, \dots, C$  required to represent the subspace of the particular face image class is selected as a function of the within-class sample variance. Specifically,  $K^{(j)}$  is set equal to  $K_0^{(j)} + \Delta K^{(j)}$ , being  $K_0^{(j)}, j = 1, \dots, C$  a set of constant values such that  $\sum_{j=1}^C K_0^{(j)} < K_C$  and

$$\Delta K^{(j)} = \left( K_C - \sum_{j=1}^C K_0^{(j)} \right) \frac{\text{tr}(\mathbf{Cov}^{(j)})}{\sum_{j=1}^C \text{tr}(\mathbf{Cov}^{(j)})}. \quad (3)$$

where  $\mathbf{Cov}^{(j)}$  denotes the covariance matrix for the  $j$ -th class

$$\mathbf{Cov}^{(j)} = \frac{1}{N} \left[ \sum_{i=1}^N (\mathbf{X}_i^{(j)} - \boldsymbol{\mu}^{(j)})(\mathbf{X}_i^{(j)} - \boldsymbol{\mu}^{(j)})^T \right] \quad (4)$$

With these positions, we now investigate the impact of dimensionality reduction in the wavelet transform domain on IA  $L_1$ -PCA. Specifically, we apply Daubechies filter with  $L_{max}$  levels of decomposition to all the class images, and consider the cases in which a restrained fraction of the DWT coefficients are retained, i.e. we set  $L = L_{max} - l$ , being  $l = 1, 2$ . We refer to this approach as Wavelet Domain Reduced (WDR) IA  $L_1$ -PCA. For comparison sake, we consider the case where all the DWT coefficients are retained, i.e.  $L = L_{max}$ , which coincides with IA  $L_1$ -PCA [5].

## 4. EXPERIMENTAL RESULTS

In this section we want to assess the resilience of IA  $L_1$ -PCA with respect to wavelet domain data reduction by comparing the performance of WDR IA  $L_1$ -PCA and IA  $L_1$ -PCA. We consider on three different database: Extended Yale Face Database, ORL Database and Aberdeen Database. For the sake of completeness, we also show the resilience of one of the major holistic competitors, i.e. the LDA algorithm [?].

As a face recognition performance metric, we here consider the average error, defined as the  $N_E(p)$  number of classification error as a function of the number  $p$  of PCs, normalized with respect to the number of classes  $C$ , the number  $N_t$  of test images per class per run, and the number of run  $N_r$ . The average error equals the probability of face misclassification:

$$P_E(p) \approx \frac{N_E(p)}{N_C \cdot N_r \cdot N_t} \quad (5)$$

The analysis is applied both on original and partially occluded test and training images. The Figs. 4-6 show examples of the occluded images and their wavelet transform considering each database; further details on the occlusion model and on the experimental settings are given in the following subsections.

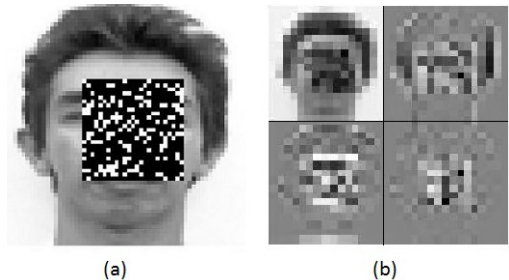


**Fig. 4.** A subject of Aberdeen database affected by partial occlusion with wavelet application.

### 4.1. Wavelet Domain Reduced (WDR) Individual Adaptive $L_1$ -PCA

#### 4.1.1. Extended Yale Face Database

We consider the Extended Yale Face database, built by  $C = 8$  classes, of 25 images each. In the following experiments, we randomly select 8 images training per class and use the remaining 17 images for testing. The image size is  $64 \times 64$  pixels<sup>1</sup>, so  $D = 4096$ , and we carried out 50 independent

<sup>1</sup>The cropped images are used.

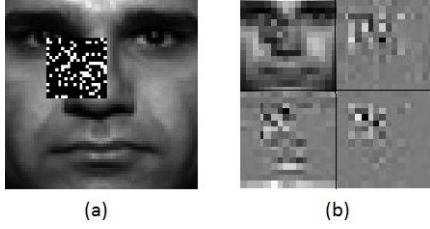


**Fig. 5.** A subject of Yale database affected by partial occlusion with wavelet application.

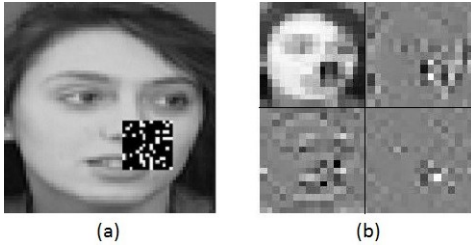


**Fig. 6.** A subject of Orl database affected by partial occlusion with wavelet application.

runs. We apply Daubechies filter, with  $L_{max} = 4$  levels of decomposition. We consider WDR IA  $L_1$ -PCA when half of the DWT coefficients are retained, i.e.  $L = L_{max} - 2$ , and compare it with IA  $L_1$ -PCA, where all the DWT coefficients are retained, i.e.  $L = L_{max}$ . In both cases, the IA  $L_1$ -PCA uses up to 48 PCs.

We consider a Percentage of Occluded Images (POI)  $p_j$ ,  $j = 1 \dots C$  of the  $j$ -th class, regardless if training or test images, to be partially occluded. In order to model random occlusions, we consider occluding patches of size  $[15 \times 15, 20 \times 20, 25 \times 25, 30 \times 30]$  pixels, filled with “salt and pepper” noise modeling random visual content of the occluded area. We set  $p_1 = p_2 = 10\%$ ,  $p_3 = p_4 = 30\%$ ,  $p_5 = p_6 = 50\%$ , and  $p_7 = p_8 = 70\%$ .

Fig.7 shows the average error of WDR IA  $L_1$ -PCA and IA  $L_1$ -PCA for the Extended Yale Face database, as a function of the number of principal components per class; for comparison sake, we report also the results achieved by  $L_1$ -PCA using up to 20 PCs in a common subspace; the algorithms are referred to as “Adaptive Individual” and “Common” in the legend. It is interesting to observe that the WDR IA  $L_1$ -PCA may outperform IA  $L_1$ -PCA, i.e. wavelet domain reduction from  $L = L_{max}$  to  $L = 2$  is even beneficial; in fact, discarding higher wavelet decomposition layers corre-

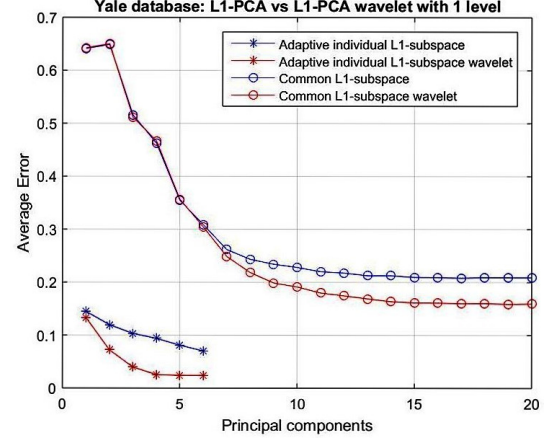


**Fig. 7.** Recognition performance of WDR IA  $L_1$ -PCA and IA  $L_1$ -PCA [5] (“Adaptive Individual”) for the Extended Yale Face database;  $L_1$ -PCA (“Common”) is also reported for comparison’s sake.

sponds to discarding less relevant visual data. This is particularly relevant for the IA  $L_1$ -PCA, that allows the most suited distribution of the PCs to each classes, and thanks to the wavelet reduction operates on data cleaned by less relevant visual details. Clearly, a tradeoff is encountered in reducing the image representation accuracy and properly characterizing the image visual features. Besides, let us notice that the selected coefficients could be further exploited by means of polynomial classification; this is left for further study [17].

#### 4.1.2. Aberdeen Database

For the Aberdeen database we have  $C = 8$  number of classes, for each class we have 18 total images, and we choose  $N = 8$  random images from each dataset for training and the remaining 10 images for testing. The dimension of each images is  $64 \times 64$  pixels, so  $D = 4096$ , and we carried out 50 independent experiments. Regarding the number of principal components we have: for the “common” subspace up to 20 PCs and for the “adaptive individual” subspace up to 48 PCs both with and without wavelet application.

We set POI as  $p_1 = p_2 = 10\%$ ,  $p_3 = p_4 = 30\%$ ,  $p_5 = p_6 = 50\%$ ,  $p_7 = p_8 = 70\%$ ; the corruption affects for both the training and testing set of each class. In addition we choose the occluding patch size in this range =  $[15 \times 15, 20 \times 20, 25 \times 25, 30 \times 30]$  pixels. In the results, we observe that the WDR version of different classifiers often outperforms the basic one. Specifically WDR “common”  $L_1$ -PCA is better than the “common”  $L_1$ -PCA and we can see there is a big gap between them. The same conclusion can be drawn for the “individual” subspace and in particular we

WDR IA $L_1$ -PCA, Aberdeen database		
PC's	$L = L_{max} - 2$	$L = L_{max}$ [5]
8	0.0668	0.0953
16	0.0597	0.0717
24	0.0520	0.0617
32	0.0468	0.0527
40	0.0462	0.0462
48	0.0430	0.0440

**Table 1.** Error rate for the WDR IA  $L_1$ -PCA subspace and the IA  $L_1$ -PCA [5] using the Aberdeen database

can see that the WDR "adaptive" method achieves a lower recognition error rate than the previous "adaptive" method.

Tab.4.1.2 shows the average error of WDR IA  $L_1$ -PCA and IA  $L_1$ -PCA for the Aberdeen database; WDR IA  $L_1$ -PCA still outperforms IA  $L_1$ -PCA.

## 4.2. LDA in wavelet domain

In this section, for comparison sake we analyze the performance of the WDR LDA algorithm and compare it with the basic LDA [16]. Specifically, we want to show the results obtained with three different database: Extended Yale Face Database, ORL Database and Aberdeen Database. In each experiment we used Daubechies filter, with length  $L_{max} = 4$ . For all the databases, we did the experiments discarding one and two levels,  $L = L_{max} - 1$ ,  $L = L_{max} - 2$ , so representing the images with 32x32 and 16x16 DWT coefficients, respectively.

### 4.2.1. Extended Yale Face Database

For the Extended Yale Face database<sup>2</sup> we have  $C = 8$  number of classes, for each class we have 25 total images and we choose  $N = 8$  random images from each dataset for training and the remaining 17 images for testing. The dimension of each images is 64x64 pixels, so  $D = 4096$ , and we carried out 50 independent experiments. Regarding the number of principal components we compute both for the WDR LDA and LDA up to 56 PC's. We add the random occluding patches in the following way: we set POI as  $p_1 = p_2 = 10\%$ ,  $p_3 = p_4 = 30\%$ ,  $p_5 = p_6 = 50\%$ , and  $p_7 = p_8 = 70\%$ ; the corruption affects both the training and testing set of each class. In addition we choose the occluding patch size in this range = [15x15, 20x20, 25x25, 30x30] pixels.

The results of the experiments on the database are shown in Table 2. The WDR LDA maintains the same performance as LDA when higher layers DWT coefficients are discarded, but a performance improvement is not observed, and WDR LDA maintains the same trends observed on the original data.

<sup>2</sup>The cropped images are used.

WDR LDA, Extended Yale Face database			
PC's	$L = L_{max} - 2$	$L = L_{max} - 1$	$L = L_{max}$ [16]
8	0.2956	0.3160	0.3196
16	0.1268	0.1275	0.1296
24	0.0656	0.0750	0.0700
32	0.0385	0.0712	0.0457
40	0.0234	0.0387	0.0301
48	0.0131	0.0238	0.0178
56	0.0034	0.0135	0.0056

**Table 2.** Error rate of WDR LDA and LDA [16] for different representation levels using the Extended Yale Face database

### 4.2.2. ORL database

For the ORL database we have  $C = 8$  number of classes, for each class we have 10 total images and we choose  $N = 7$  random images from each dataset for training and the remaining 3 images for testing. The dimension of each images is 64x64 pixels, so  $D = 4096$ , and we carried out 50 independent experiments. Regarding the number of principal components we compute both for the WDR LDA and LDA up to 56 PC's. We set POI as  $p_1 = p_2 = 30\%$ ,  $p_3 = p_4 = 40\%$ ,  $p_5 = p_6 = 60\%$ ,  $p_7 = p_8 = 80\%$ ; occlusions affects both the training and testing set of each class. In addition we choose the occluding patch size in this range = [25x25, 30x30, 35x35, 40x40] pixels.

In Table 3, we recognize that the wavelet domain reduction does not affect the LDA performance, and may even be beneficial, since it provides a compact representation.

### 4.2.3. Aberdeen Database

For the Aberdeen database we have  $C = 8$  number of classes, for each class we have 18 total images and we choose  $N = 8$  random images from each dataset for training and the remaining 10 images for testing. The dimension of each images is 64x64 pixels, so  $D = 4096$ , and we carried out 50 independent experiments. Regarding the number of principal components we compute both for the LDA and LDA with wavelet up to 56 PC's. We set  $p_1 = p_2 = 10\%$ ,  $p_3 = p_4 = 30\%$ ,  $p_5 = p_6 = 50\%$ ,  $p_7 = p_8 = 70\%$ , both on the training and testing set of each class. In addition we choose the occluding patch size in this range = [15x15, 20x20, 25x25, 30x30] pixels.

Table 4 confirms the already observed trends, in that the WDR LDA maintains the same performance as LDA when higher layers DWT coefficients are discarded.

## 5. CONCLUSION AND FURTHER WORK

In this work, we tackled the problem of cloud-assisted IA  $L_1$ -PCA face recognition using wavelet-domain compressed



<b>WDR LDA, ORL database</b>			
PC's	$L = L_{max} - 2$	$L = L_{max} - 1$	$L = L_{max}$ [16]
8	0.3917	0.3783	0.4275
16	0.2075	0.1833	0.2383
24	0.1133	0.0975	0.1383
32	0.0675	0.0558	0.0775
40	0.0442	0.0267	0.0492
48	0.0275	0.0192	0.0342
56	0.0117	0.0075	0.0175

**Table 3.** Error rate of WDR LDA and LDA [16] for different representation levels using the ORL database

<b>WDR LDA, Aberdeen database</b>			
PC's	$L = L_{max} - 2$	$L = L_{max} - 1$	$L = L_{max}$ [16]
8	0.4303	0.4325	0.4397
16	0.2170	0.2223	0.2507
24	0.1068	0.1098	0.1407
32	0.0585	0.0560	0.0850
40	0.0325	0.0315	0.0488
48	0.0150	0.0190	0.0275
56	0.0092	0.0098	0.0275

**Table 4.** Error rate of WDR LDA and LDA [16] for different representation levels using the Aberdeen database

images. Specifically, we analyzed the impact of wavelet domain image compression on the Individual Adaptive (IA)  $L_1$ -PCA subspace computation and assess the performance of a classifier operating on data characterized by increasing compactness and accordingly decreasing accuracy. We established that IA  $L_1$ -PCA classification is resilient to data reduction performed in the wavelet domain. This result, confirmed also for others state-of-the-art competitors, paves the way for designing a classification architecture in which smart wireless devices upload simplifying data and offload the classification stage to a server in the cloud. Further work will focus on the impact of different pre-processing techniques as well as of different encoding techniques, e.g. compressive sampling, at the mobile device on the performance of the cloud-based classification stage.

## 6. REFERENCES

- [1] W. Zhao, R. Chellappa, P.J. Phillips, A. Rosenfeld, "Face recognition: A literature survey", *ACM computing surveys (CSUR)*, 35(4), 399-458.
- [2] P.Markopoulos, G. Karystinos, D. Pados, "Optimal Algorithms for L1 subspace Signal Processing" *IEEE Transactions on Signal Processing*, 62, 5046-5058.
- [3] P. P. Markopoulos, S. Kundu and D. A. Pados, "L1-fusion: Robust linear-time image recovery from few severely corrupted copies," *Image Processing (ICIP), 2015 IEEE International Conference on*, Quebec City, QC, 2015, pp. 1225-1229.
- [4] M. Pierantozzi, Y. Liu, S. Colonnese and D. A. Pados, "Video background tracking and foreground extraction via L1-subspace updates", *Proc. SPIE 9857, Compressive Sensing V: From Diverse Modalities to Big Data Analytics*, May 2016.
- [5] F. Maritato, Y. Liu, S. Colonnese and D. A. Pados, "Face recognition with  $L_1$ -norm subspaces", *Proc. SPIE 9857, Compressive Sensing V: From Diverse Modalities to Big Data Analytics*, May 2016.
- [6] S.Colonnese, F., Cuomo, T., Melodia, R., Guida, "Cloud-assisted buffer management for HTTP-based mobile video streaming", PE-WASUN 2013 { Proc. of the 10th ACM Symposium on Performance Evaluation of Wireless Ad Hoc, Sensor, and Ubiquitous Networks.
- [7] O. Atan, Y. Andreopoulos, C. Tekin and M. van der Schaar, "Bandit Framework for Systematic Learning in Wireless Video-Based Face Recognition", in *IEEE Journal of Selected Topics in Signal Processing*, vol. 9, no. 1, pp. 180-194, Feb. 2015
- [8] T.Soyata, R. Muraleedharan, C. Funai, M. Kwon, W. Heinzelman, "Cloud-vision: Real-time face recognition using a mobile-cloudlet-cloud acceleration architecture", *Computers and Communications (ISCC), 2012 IEEE Symposium on* .
- [9] A.Grossmann, J.Morlet, "Decomposition of Hardy functions into square integrable wavelets of constant shape", *SIAM Journal on Mathematical Analysis* 15.4, 1984.
- [10] A. Skodras, C. Christopoulos, and T. Ebrahimi, "The JPEG 2000 Still Image Compression Standards and Beyond", *IEEE Transactions on Circuits and Systems for Video Technology*, Vol. 8, No. 7, pp. 814-837, November 1998.
- [11] I. Ram, I. Cohen and M. Elad, "Facial Image Compression using Patch-Ordering-Based Adaptive Wavelet Transform", *IEEE Signal Processing Letters*, vol. 21, no. 10, pp. 1270-1274, Oct. 2014.
- [12] K. Etemad, Rama Chellappa, "Discriminant analysis for recognition of human face images", *J. Opt. Soc. Am. A/* Vol. 14, No. 8/ August 1997.
- [13] Dao-Qing Daia, P.C. Yuenb, "Wavelet based discriminant analysis for face recognition" *Applied Mathematics and Computation*, Vol. 175, no. 1, 1 April 2006, Pages 307-318.
- [14] B.E. Usevitch, "A tutorial on modern lossy wavelet image compression: foundations of JPEG 2000," *IEEE Signal Processing Magazine*, vol.18, no.5, September 2001.
- [15] E. Gumus, N. Kilic, A. Sertbas, O. N. Ucan, "Evaluation of face recognition techniques using PCA, wavelets and SVM", *Expert Systems with Applications*, Vol.37, no. 9, September 2010.
- [16] D. Cai, X. He and J. Han, "SRDA: An Efficient Algorithm for Large-Scale Discriminant Analysis," *IEEE Transactions on Knowledge and Data Engineering*, vol. 20, no. 1, pp. 1-12, Jan. 2008.
- [17] G. Scarano, L. Forastiere, S. Colonnese, S. Rinauro, "Reduced polynomial classifier using within-class standardizing transform", *Int. Symp. on Comm. Control and Signal Proc.*, ISCCSP 2012.